III. 研究成果の刊行に関する一覧表

研究成果の刊行に関する一覧表

書籍

著者氏名	論文タイトル名	書籍全体の編集者名	書　籍　名	出版社名	出版地	出版年	ページ
服部英幸	ＢＰＳＤに応じた対応	小長谷陽子	本人・家族のための若年性認知症サポートブック	中央法規	東京	2010	191-199
遠藤英俊		遠藤英俊	高齢者への服薬指導Ｑ＆Ａ	医薬ジャーナル社	大阪	2010	203頁
遠藤英俊	9－2－5　認知症　第９章　精神科医療	精神保健福祉白書編集委員会	精神保健福祉白書　２０１１年版　岐路に立つ精神保健医療福祉―新たな構築をめざして	中央法規出版		2010	全 217頁 (P149)
遠藤英俊	高齢者の薬物療法	山口徹、北原光夫、福井次矢	今日の治療指針	医学書院	東京	2011	1387-1396

雑誌

発表者氏名	論文タイトル名	発表誌名	巻号	ページ	出版年
Takamura A, Okamoto Y, Kawarabayashi T, Yokoseki T, Shibata M, Mouri A, Nabeshima T, Sun H, Abe K, Shoji M, Yanagisawa K, Michikawa M, Matsubara E	Extracellular and intraneuronal HMW-AβOs represent a molecular basis of memory loss in Alzheimer's disease model mouse.	**Mol Neurodegener**	6	20	2011
Takamura A, Kawarabayashi T, Yokoseki T, Shibata M, Morishima-Kawashima M, Saito Y, Murayama S, Ihara Y, Abe K, Shoji M, Michikawa M, Matsubara E	Dissociation of β-amyloid from Lipoprotein in Cerebrospinal Fluid from Alzheimer's Disease accelerates β-amyloid-42 assembly.	J Neurosci Res	In press		2011

Wakasaya Y, Kawarabayashi T, Watanabe M, Yamamoto-Watanabe Y, Takamura A, Kurata T, Murakami T, Abe K, Yamada K, Wakabayashi K, Sasaki A, Westaway D, Hyslop PS, Matsubara E, Shoji M	Factors responsible for neurofibrillary tangles and neuronal cell losses in tauopathy.	**J Neurosci Res.**	89	576-584	2011
Seino Y, Kawarabayashi T, Wakasaya Y, Watanabe M, Takamura, A, Yamamoto-Watanabe Y, Kurata T, Abe K, Ikeda M, Westaway D, Murakami T, St.George-Hyslop P, MatsubaraE, Shoji M	Aβ amyloid accelerates phosphorylation of tau and NFT formation in APP and tau double transgenic mice model.	**J Neurosci Res.**	88	3547-3554	2010
Matsuno K, Takai K, Isaka Y, Unno Y, Sato M, Takikawa O, Asai A	S-benzylisothiourea derivatives as small-molecule inhibitors of IDO.	**Bioorg Med Chem Lett.**	20	5126-5129	2010
滝川　修、横山祐一	Indoleamine 2,3-dioxygenase (IDO)の病態生理学的意義と阻害剤の開発	ファルマシア(日本薬学会誌)	46	241-246	2010
Hiramoto M, Maekawa N, Kuge T, Ayabe F, Watanabe A, Masaike Y, Hatakeyama M, Handa H, Imai T	High-performance affinity chromatography method for identification of L-arginine interacting factors using magnetic nanobeads.	**Biomed. Chromatogr**	24	606-612	2010
Takahashi K, Adachi K, Kunimoto S, Wakita H, Takeda K, Watanabe A	Potent inhibitors of amyloid ß fibrillization, 4,5-dianilinophthalimide and staurosporine aglycone, enhance degradation of preformed aggregates of mutant Notch3.	**Biochem. Biophys. Res. Commun**	402	54-58	2010

Nishitsuji K, Hosono T, Uchimura K, Michikawa M.	Lipoprotein Lipase Is a Novel Amyloid β (Aβ)-binding Protein That Promotes Glycosaminoglycan-dependent Cellular Uptake of Aβ in Astrocytes	**J Biol Chem**	286	6393-6401	2011
Akatsu H, Ogawa N, Kanesaka T, Hori A, Yamamoto T, Matsukawa N, Makoto Michikawa	Higher activity of peripheral blood angiotensin-converting enzyme is associated with later-onset of Alzheimer's disease	**J Neurosci Res**	300	67-73	2011
Minagawa H, Watanabe A, Akatsu H, Adachi K, Ohtsuka C, Terayama Y, Hosono T, Takahashi S, Wakita H, Jung CG, Komano H, Michikawa M.	Homocysteine, another risk factor for Alzheimer's disease, impairs apolipoprotein E3 function.	**J Biol Chem**	285	38382-38388	2010
服部英幸	高齢者うつ病は認知症とどこが違うのか－対処法は？	訪問看護と介護	15(1)	32-38	2010
服部英幸、森明子、小長谷陽子、鈴木亮子	デイケア利用者におけるうつの実態とデイケアの効果	日本医事新報	4472	93-96	2010
服部英幸	認知症の地域医療-各医療機関の特性（得手不得手）と地域連携の現状・課題４）老年医療専門病院の認知症専門医としての立場から	神経内科 Suppl.6	72	206-210	2010

Hideyuki Hattori, Kenji Yoshiyama, Rina Miura, Sachiko Fujie	Clinical psychological tests useful for differentiating depressive state with Alzheimer's disease from major depression of the elderly.	**PSYCHOGERI-ATRICS**	10	29-33	2010
服部英幸	高齢者在宅医療の実際 3) 認知症への対応	**Geriatric Medicine**	48	1511-1517	2010
服部英幸	Can an individualized and comprehensive care strategy improve urinary incontinence (UI) among nursing home residents?	**Arch Gerontol Geriatr**	49(2)	278-283	2009
遠藤英俊	後期高齢者医療と老年医学	日本老年医学会雑誌	47(2)	95-100	2010
遠藤英俊、佐竹昭介、三浦久幸	［各論］認知症	臨床スポーツ医学	27(11)	1247-1249	2010
遠藤英俊、三浦久幸	特集　認知症治療の今後を予測する　1.認知症治療の現状と今後	医薬ジャーナル	46(5)	67-71	2010
遠藤英俊、木之下徹、永田久美子、東海林幹夫、田口真源	特集Ⅰ認知症・BPSDの医療とケアの今	Science of Kanpo Medicine 漢方医学	34(2)	94(8)-106(20)	2010
遠藤英俊、三浦久幸	社会的・制度的支援と家族介護　1）介護保険	神経内科	72(Suppl.6)	217-221	2010
遠藤英俊、佐竹昭介、洪 英在、田代真耶子、三浦久幸、近藤真由	認知症の新しい治療 2.音楽療法	内科系総合雑誌 モダンフィジシャン	30(9)	1169-1172	2010
鷲見幸彦	認知症診療マニュアル．認知症患者ケアの予防的側面.	神経内科	72(6)	34-39	2010
鷲見幸彦、加藤隆司	目で見る症例．アルツハイマー型認知症.	内科	105(3)	496-500	2010

鷲見幸彦	内科疾患の診断基準病型分類重症度．アルツハイマー型認知症.	内科	105(6)	1326-1330	2010
鷲見幸彦	認知症における地域連携の重要性と問題点	医療の広場	50(12)	4-7	2010
Takahashi K, Adachi K, Yoshizaki K, Kunimoto S, Kalaria RN, Watanabe, A.	Mutations in Notch3 cause the formation and retention of aggregates in the endoplasmic reticulum, leading to impaired cell proliferation.	**Hum. Mol. Genet**	19	79-89	2010
Hiramoto M, Maekawa N, Kuge T, Ayabe F, Watanabe A, Masaike Y, Hatakeyama M, Handa H, Imai T.	High-performance affinity chromatography method for identification of L-arginine interacting factors using magnetic nanobeads.	**Biomedical Chromatography**			2010 (in press)
Takahashi K, Adachi K, Yoshizaki K, Kunimoto S, Kalaria RN, Watanabe, A.	Mutations in Notch3 cause the formation and retention of aggregates in the endoplasmic reticulum, leading to impaired cell proliferation.	**Hum. Mol. Genet**	19	79-89	2010
Yamada A, Akimoto H, Kagawa S, Guillemin GJ, Takikawa O.	Proinflammatory cytokine interferon-gamma increases indoleamine 2,3-dioxygenase in monocytic cells primed with amyloid beta peptide 1-42: Implications for the pathogenesis of Alzheimer's disease.	**J. Neurochem.**	110	791-800	2009
Nisapakultorn K, Makrudthong J, Sa-Ard-Iam N, Rerkyen P, Mahanonda R, Takikawa O.	Indoleamine 2,3-dioxygenase expression and regulation in chronic periodontitis.	**J. Periodontol.**	80	289-297	2009

Ogasawara N, Oguro T, Sakabe T, Matsushima M, Takikawa O, Isobe K, Nagase F.	Hemoglobin induces the expression of indoleamine 2,3-dioxygenase in dendritic cells through the activation of PI3K, PKC, and NF-kappaB and the generation of reactive oxygen species.	**J. Cell Biochem.**	108	716-725	2009
Brenk M, Scheler M, Koch S, Neumann J, Takikawa O, Häcker G, Bieber T, von Bubnoff D.	Tryptophan deprivation induces inhibitory receptors ILT3 and ILT4 on dendritic cells favoring the induction of human CD4+CD25+ Foxp3+ T regulatory cells.	**J. Immunol.**	183	145-154	2009
滝川 修、 横山祐一	Indoleamine 2,3-dioxygenase (IDO)の病態生理学的意義と阻害剤の開発	ファルマシア			2009 (in press)
Kim HJ, Jung CG, Dukala D, Bae H, Kakazu R Wollmann R Soliven B.	Fingolimod and related compounds in a spontaneous autoimmune polyneuropathy	**J Neuroimmunol**	214	93-1000	2009
Nakamura T, Watanabe A, Fujino T, Hosono T, and Michikawa M	Apolipoprotein E4 (1-272) fragment is associated with mitochondrial proteins and affects mitochondrial function in neuronal cells.	**Mol. Neurodegener**	4(35)	35	2009
Zou K, Maeda T, Oba R, Komano H, and Michikawa M	Aβ42-to-Aβ40- and angiotensin- converting activities in different domain of angiotensin-converting enzyme.	**J. Biol. Chem.**,	284	31914-31920	2009
Tesseur I, Brecht W, Corn J, Gong J-S, Yanagisawa K, Michikawa M, Weisgraber K, Huang Y, and Wyss-Coray T.	Bioactive TGF-β can associate with lipoproteins and is enriched in those containing apolipoprotein E3.	**J. Neurochem**	110(4)	1254-1262	2009

Doi Y, Mizuno T, Maki Y, Jin S, Mizoguchi H, Ikeyama M, Doi M, Michikawa M, Takeuchi H, and Suzumura A.	Microglia activated with toll-like receptor 9 ligand CpG attenuate oligomeric amyloid-β neurotoxicity in vitro and in vivo models of Alzheimer's disease.	**Am. J. Pathol.**	175	2121-2132	2009
Maeda T, Marutani T, Zou K, Araki W, Yagishita N, Yamamoto Y, Amano T, Michikawa M, Nakajima T, and Komano H	An E3 ubiquitin ligase, Synoviolin is involved in the degradation of immature Nicastrin, and regulates the production of amyloid b-protein.	**FEBS J**	276	5832-5840	2009
Minagawa K, Gong J-S, Jung C-G, Watanabe A, Lund-Katz S, Phillips M C, Saito H, and Michikawa M.	Mechanism underlying apolipoprotein E isoform-dependent lipid efflux from neural cells in culture.	**J. Neurosci. Res.**	87	2498-2508	2009
Kasahara E, Kashiba M, Jikumaru M, Kuratsune D, Orita K, Yamate Y, Hara K, **Sekiyama A,** Sato EF, Inoue M	Dynamic aspects of ascorbic acid metabolism in the circulation: analysis by ascorbate oxidase with a prolonged in vivo half-life.	**Biochem J.**	421(2)	293-296	2009
伊藤健吾　加藤隆司	FDG-PETによるアルツハイマー病の早期診断	**Dementia Japan**	23	14-21	2009
伊藤健吾　加藤隆司	認知症の診断と根本治療薬の開発に貢献するPETイメージング	**日本神経精神薬理雑誌**	29	153-160	2009

IV. 研究成果の刊行物・別刷

Journal of Neuroscience Research 00:000–000 (2011)

Dissociation of β-Amyloid From Lipoprotein in Cerebrospinal Fluid From Alzheimer's Disease Accelerates β-Amyloid-42 Assembly

Ayumi Takamura,[1,2] Takeshi Kawarabayashi,[2] Tatsuki Yokoseki,[3] Masao Shibata,[3] Maho Morishima-Kawashima,[4] Yuko Saito,[5] Shigeo Murayama,[5] Yasuo Ihara,[6] Koji Abe,[7] Mikio Shoji,[2] Makoto Michikawa,[1] and Etsuro Matsubara[1,2]*

[1]Department of Alzheimer's Disease Research, Research Institute, National Center for Geriatrics and Gerontology, Aichi, Japan
[2]Department of Neurology, Institute of Brain Science, Hirosaki University Graduate School of Medicine, Aomori, Japan
[3]Immunas Pharma Inc., Kanagawa, Japan
[4]Department of Molecular Neuropathology, Faculty of Pharmaceutical Sciences, Hokkaido University, Hokkaido, Japan
[5]Department of Neuropathology, Tokyo Metropolitan Institute of Gerontology, Tokyo, Japan
[6]Department of Neuropathology, Faculty of Life and Medical Sciences, Doshisha University, Kyoto, Japan
[7]Department of Neurology, Okayama University School of Medicine, Okayama, Japan

Monoclonal 2C3 specific toβ-amyloid (Aβ) oligomers (AβOs) enabled us to test our hypothesis that the alteration of lipoprotein–Aβ interaction in the central nervous system (CNS) initiates and/or accelerates the cascade favoring Aβ assembly. Immunoprecipitation of frontal cortex employing 2C3 unequivocally detected soluble 4-, 8-, and 12-mers in Alzheimer's disease (AD) brains. Immunoblot analysis of the entorhinal cortex employing 2C3 revealed that the accumulation of soluble 12-mers precedes the appearance of neuronal loss or cognitive impairment and is enhanced as the Braak neurofibrially tangle (NFT) stages progress. The dissociation of soluble Aβ from lipoprotein particles occurs in cerebrospinal fluid (CSF), and the presence of lipoprotein-free oligomeric 2C3 conformers (4- to 35-mers) was evident, which mimic CNS environments. Such CNS environments may strongly affect conformation of soluble Aβ peptides, resulting in the conversion of soluble $A\beta_{42}$ monomers into soluble $A\beta_{42}$ assembly. The findings suggest that functionally declined lipoproteins may accelerate the generation of metabolic conditions leading to higher levels of soluble $A\beta_{42}$ assembly in the CNS.

Key words: Alzheimer's disease; Aβ; lipoprotein; oligomer; monomer

Accumulating lines of evidence indicate that memory loss represents a synaptic failure caused directly by soluble β-amyloid (Aβ) oligomers (AβOs; Klein et al., 2001; Selkoe, 2002; Hass and Selkoe, 2007). The possible mechanism underlying the neurotoxic action of AβOs has been postulated as neurotoxic ligands (Lambert et al., 1998; Walsh et al., 2002; Chromy et al., 2003; Gong et al., 2003; Lacor et al., 2004; Cleary et al., 2005; Lesné et al., 2006; Shankar et al., 2008; Noguchi et al., 2009), iron channel formation (Lin et al., 2001; Quist et al., 2005), pore formation (Lashuel et al., 2002; Kayed et al., 2009), and dysfunction of cholesterol metabolism in neurons (Michikawa et al., 2001; Gong et al., 2002; Zou et al., 2002). However, the exact metabolic conditions controlling the in vivo generation of soluble AβOs remain unknown. It is well known that aging is the most prevailing risk factor for sporadic AD. In vivo studies have shown that Aβ neurotoxicity is closely related to the brain aging via unknown age-related factors (Geula et al., 1998), perhaps reflecting metabolic alterations. Notably, the APOE genotype is also the major genetic risk factor for late-onset sporadic AD (Schmechel et al., 1993; Tanzi and Bertram, 2001; Wellington, 2004). HDL-like lipoproteins, mainly

Contract grant sponsor: Ministry of Education, Culture, Sports, Science and Technology, Japan (to E.M.); Contract grant sponsor: the Program for Promotion of Fundamental Studies in Health Sciences of the National Institute of Biomedical Innovation (NIBIO; to E.M.).

*Correspondence to: Etsuro Matsubara, Department of Neurology, Institute of Brain Science, Hirosaki University Graduate School of Medicine, 5 Zaifu, Hirosaki, Aomori 036-8216, Japan. E-mail: etsuro@cc.hirosaki-u.ac.jp

Received 7 September 2010; Revised 17 December 2010; Accepted 11 January 2011

Published online 00 Month 2011 in Wiley Online Library (wileyonlinelibrary.com). DOI: 10.1002/jnr.22615

lipidated apoE, are in charge of cholesterol transport to and from neurons (Michikawa et al., 2001; Gong et al., 2002), in which cholesterol metabolism is quite different from that in systemic circulation. In addition to lipid trafficking, apoE as a form of HDL-like lipoprotein plays a major role in Aβ metabolism in the central nervous system (CNS). Under physiological conditions, HDL-like lipoproteins unequivocally interact with soluble Aβ in cerebrospinal fluid (CSF; Koudinov et al., 1996). Interestingly, when the generation of HDL-like lipoproteins in the AD mouse model is suppressed or overexpressed via the specific regulation of ATP-binding cassette A1 (ABCA1), Aβ deposition exhibits augmentation or reduction, respectively, which depends on the degree of ABCA1-mediated lipidation of apoE in the CNS (Wahrle et al., 2005, 2008). From these points of view, lipidic environments in the CNS represent one of the prevailing metabolic conditions. We hypothesized that an alteration of the lipoprotein–sAβ interaction in the CNS is capable of initiating and/or accelerating the cascade favoring Aβ assembly. Actually, we demonstrate that functionally declined lipoproteins may be the major determinants in the generation of metabolic conditions leading to higher levels of the soluble dimeric form of Aβ in AD brains (Matsubara et al., 1999, 2004). To verify this hypothesis and extend previous observations (Matsubara et al., 1999, 2004), we focused on the entorrhinal cortex (EC) as well as CSF, which mimics CNS environments, followed by biochemical analyses using an antioligomer specific antibody. The presence of lipoprotein-free soluble AβOs in CSF was assessed in age-matched normal controls (NCs) and patients with Alzheimer's disease (AD) by size-exclusion chromatography (SEC) and enzyme-linked immunosorbent assay (ELISA) specific for either AβOs or AβMs to test our hypothsis.

MATERIALS AND METHODS

Generation of Monoclonal 2C3

Monoclonal 2C3, which is specific to AβOs with a molecular mass larger than tetramers (unpublished data), was generated and characterized as described elsewhere.

Patients

CSF samples (5 ml) were collected from 13 age-matched normal controls (NCs; 70.6 ± 8.2 years old) and 12 AD patients (73.2 ± 7.8 years old) after 12 hr of fasting. None of the individuals in the two groups had a history of stroke or other neurological conditions in the CNS that might have affected their lipoprotein profile, and none was taking drugs known to affect lipid metabolism. The diagnosis of AD was made in accordance with the NINCDS-ADRDA criteria, and only those who met the criteria of probable AD were included.

Lipoprotein Separation and Depletion

After separation of CSF collected from 12 patients with AD and 13 NCs, lipoprotein depletion was carried out by preparative sequential density flotation ultracentrifugation using 600 μl of CSF and a protocol previously described (Matsubara et al., 2004). Briefly, the density of the collected CSF was adjusted to 1.25 g/ml using KBr, and the CSF was ultracentrifuged at 100,000 rpm for 8 hr at 16°C using a Hitachi RP100AT rotor. The infranatant at a density of 1.25 g/ml, named *lipoprotein-depleted CSF* (LPD-CSF), and the floated lipoproteins were subjected to ultrafiltration using a 3-kDa cutoff membrane (Microcon 3; Amicon, Inc.) and stored either frozen or at 4°C until use.

SEC

SEC (molecular exclusion, 2×10^6; void volume varied from fraction (Fr.) 7 to Fr. 9 enabled us to separate specifically not only AβMs from AβOs, but also lipoprotein-associated Aβ from lipoprotein-free Aβ, as previously reported (Matsubara et al., 2004). The Aβ species either in whole CSF or in lipoprotein-depleted CSF were fractionated on a Superose 12 size-exclusion column (1 cm × 30 cm; Pharmacia, Uppsala, Sweden) equilibrated with the corresponding mobile-phase solution at a flow rate of 0.5 ml/min. Twenty-eight fractions of 1 ml each were collected and analyzed. Lipoprotein was depleted as described previously (Matsubara et al., 2004). Details are also described below. To determine where Aβ eluted, a 100-μl aliquot from each fraction was analyzed in a BNT77-BC05 or BNT77-BA27 enzyme-linked immunosorbent assay (ELISA) as described previously in detail (Matsubara et al., 2004). For evaluation of lipids, total cholesterol levels were enzymatically measured using a standard kit (Wako, Osaka, Japan). Under our experimental conditions, CSF lipoproteins were eluted in Frs. 7–14, whereas Frs. 15–28 contained cholesterol-free proteins. To determine further where the Aβ oligomers eluted, a 100-μl aliquot from each fraction was analyzed by 2C3-based oligomer sandwich ELISA.

Human Tissue Subjects and Extractions

The current study is based on autopsy cases (n = 50; 26 men, 24 women) from the Brain Bank at the Tokyo Metropolitan Institute of Gerontology (Itabashi, Tokyo, Japan). All of the subjects and the sampling methods were reported previously in detail (Katsuno et al., 2005). In this project, we focused on the soluble brain fraction, which was not characterized in a previous study (Katsuno et al., 2005). Briefly, frozen tissue samples (the anterior portion of the entorhinal cortex) were homogenized in 9 volumes of Tris-saline (TS) buffer containing a cocktail of protease inhibitors as described previously (Katsuno et al., 2005). The homogenates were centrifuged at 265,000*g* for 20 min. One-third (0.5 ml) of the homogenates was subjected to 2C3 immunoblot analysis.

ELISA Specific for Either AβMs or AβOs in CSF

After informed consent had been obtained, CSF samples were collected and stored in the human resource bank of the Department of Neurology, Okayama University School of Medicine. All human age-matched CSF samples were randomly selected from this bank and used for this study. To characterize the presence of AβOs in CSF, the CSF samples were subjected to SEC as described above. To determine

where Aβ was eluted, 100-μl fractions were analyzed by AβM-specific BNT77-BA27 or BNT77-BC05 ELISA as described previously in detail (Matsubara et al., 2004). With regard to ELISA specific for AβOs, a chemiluminescence-based ELISA was carried out to detect specifically AβOs, not monomeric Aβ. Microplates (Maxisorp White Microplate; Nunc, Roskilde, Denmark) were precoated with monoclonal 2C3 (IgG2b isotype) and sequentially incubated for 24 hr at 4°C with 100 μl of different samples, followed by 24-hr incubation at 4°C with horseradish-peroxidase-conjugated BA27 Fab′ fragment (anti-$Aβ_{1–40}$ antibody, specific for $Aβ_{40}$; Wako) or horseradish-peroxidase-conjugated BC05 Fab′ fragment (anti-$Aβ_{35–43}$ antibody, specific for $Aβ_{42}$, Wako). Chemiluminescence was developed using SuperSignal ELISA Pico Chemiluminescent substrate (Pierce, Rockford, IL) on a Veritas microplate luminometer (Promega, Madison, WI).

Human Materials Including Brain and CSF

All human brains were used under a protocol provided by the human studies committee for research-related use of human materials of the Faculty of Medicine, University of Tokyo; Tokyo Metropolitan Institute of Gerontology; Tokyo Metropolitan Geriatric Hospital; and National Center for Geriatrics and Gerontology. This research project was approved by the local ethical committee of the Faculty of Medicine, University of Tokyo; Tokyo Metropolitan Institute of Gerontology; Tokyo Metropolitan Geriatric Hospital; and National Center for Geriatrics and Gerontology.

Statistical Analyses

We used factorial design analysis of variance (ANOVA) or Student's unpaired *t*-test to analyze data as appropriate. Significant ANOVA values were subsequently subjected to analyses of simple main effects or post hoc comparisons of individual means using Tukey's or Dunnett's method as appropriate. We considered $P \leq 0.05$ as significant for all studies.

RESULTS AND DISCUSSION

We determined the ability of monoclonal 2C3 to capture Aβ oligomers in AD-affected brains. Multiple "saline-soluble" Aβ species with molecular masses corresponding to those of 1-, 2-, 4-, 8-, and 12-mers were immunoprecipitated using monoclonal 6E10 from the cerebral cortex of the AD brain (Fig. 1A, lane 1). In contrast, monoclonal 2C3 unequivocally retrieved "soluble" 4-, 8-, and 12-mers from the AD brain (Fig. 1A, lane 2), but not those from the control brain (Fig. 1A, lane 3) under the conditions studied. These findings clearly demonstrated that monoclonal 2C3 is specific to AβOs, not AβMs.

Among the soluble oligomers identified, 12-mer has been shown as a candidate Aβ assembly responsible for plaque-independent cognitive decline in AD (Lesné et al., 2006). We then assessed the levels of 12-mer in saline-soluble fractions by immunoblotting using monoclonal 2C3 in 50 autopsy cases as previously reported (Katsuno et al., 2005): the entorhinal cortices (ECs) were obtained from two AD individuals, 35 individuals with Braak NFT stages I–II, and 13 individuals with Braak NFT stages III–IV. As depicted in Figure 1B, approximately 45% and 60% levels of 12-mer (AD cases,

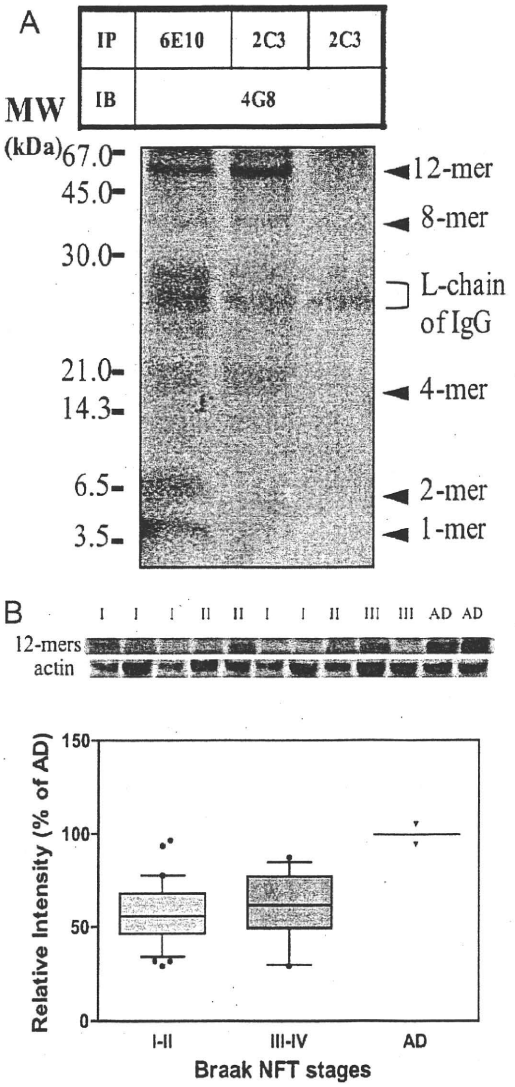

Fig. 1. Soluble oligomeric 2C3 conformers exist in human brain. **A**: 4G8 immunodetection of 6E10 or 2C3 immunoprecipitates in saline-soluble AD brain (lanes 1, 2) and control brain (lane 3). **B**: Relative intensity (percentage AD) of soluble 2C3-immunoreactive 12-mer in human entorhinal cortices obtained from 50 autopsy cases from the general aged population (Braak NFT stages I–II, n = 35; Braak NFT stages III–IV, n = 13, Braak NFT stages > IV, AD cases, n = 2).

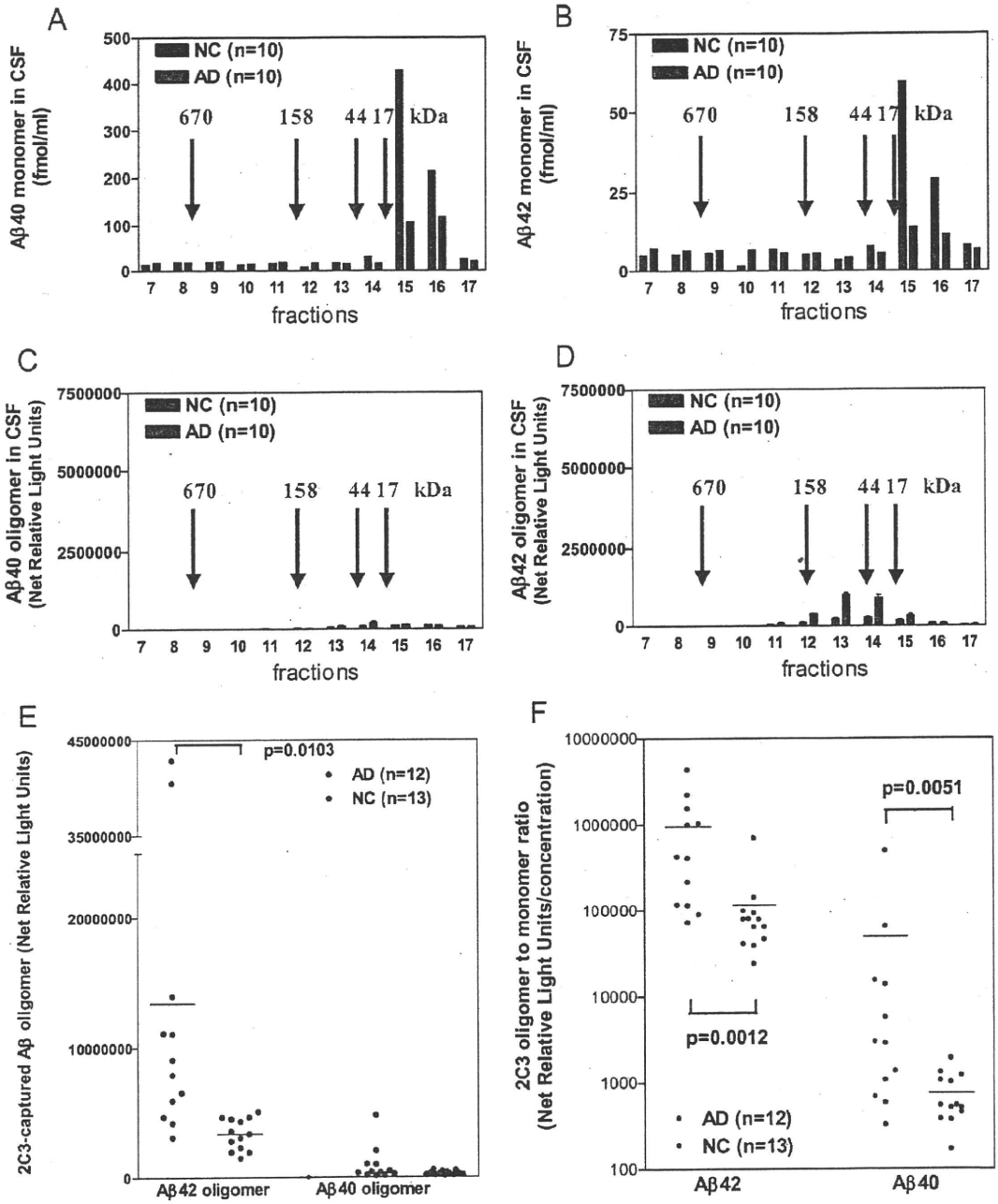

COLOR

Fig. 2. Characterization of soluble oligomeric 2C3 conformers in human CSF. The presence of AβMs was analyzed by size-exclusion chromatography (SEC) using pooled whole CSF (A,B): $Aβ_{x–40}$ monomers (**A**) vs. $Aβ_{x–42}$ monomers (**B**). The presence of AβOs was analyzed by SEC using pooled lipoprotein-depleted CSF (C,D): $Aβ_{x–40}$ oligomers (**C**) vs. $Aβ_{x–42}$ oligomers (**D**). **E**: Quantitation of oligomeric 2C3 conformers measured in 12 AD patients (red circles) and 13 NC subjects (blue circles). **F**: $Aβ_{42}$ O/M index vs. $Aβ_{40}$ O/M index. Horizontal bars indicate the mean values. The statistical significance in comparison with the age-matched control group was analyzed by the Mann-Whitney test.

J_ID: Z3P Customer A_ID: 2010-Sep-3873.R1 Cadmus Art: JNR22615 Date: 17-FEBRUARY-11 Stage: I Page: 5

100%) had already accumulated in the ECs from NCs (Braak NFT stages I–II) and in those with mild cognitive impairment (Braak stages III–IV), respectively, suggesting that the accumulation of 12-mer precedes the appearance of cognitive impairment and increases as the Braak NFT stages progress. These findings clearly showed that the ECs of AD patients exhibit metabolic conditions that accelerate Aβ assembly.

To assess further the disease-related metabolic conditions, we focused on CSF, which mimics CNS environments. By a novel 2C3-based ELISA specific for sAβOs and BNT77-based ELISAs specific for sAβMs (Enya et al., 1999; Funato et al., 1999), we directly evaluated the disease-related metabolic conditions in CSF. To investigate the presence of native sAβOs, pooled, native, whole CSF (Fig. 2A,B) and pooled lipoprotein-depleted CSF (Fig. 2C,D) were subjected to SEC. Total cholesterol was detected in whole CSF fractions 7–14, indicative of lipoprotein-associated fractions. BNT77-based ELISAs revealed that the levels of lipoprotein-associated AβMs (fractions 7–14) in AD were similar to normal control levels (Fig. 2A,B), whereas the levels of lipoprotein-free $A\beta_{x-40}$ monomers (Fig. 2A) and $A\beta_{x-42}$ monomers (Fig. 2B) in native whole CSF were lower in AD than in age-matched normal controls. In contrast, ELISA of the oligomeric 2C3 conformer in pooled, lipoprotein-depleted CSF revealed the presence of larger Aβ species in fractions 12–15 with molecular masses ranging from 17 to 158 kDa, corresponding to 4- to-35-mers (Fig. 2C,D). The levels of the oligomeric 2C3 conformer in each fraction appeared to be higher in AD patients than in normal controls. To assess further the pathological relevance of this finding, the oligomeric 2C3 conformer was measured in 12 AD patients and 13 NCs. To address the issue on the presence of any metabolic conditions favoring Aβ assembly, AβMs were also measured to evaluate the AβOs/AβMs ratio (the O/M index). Interestingly, the levels of oligomeric 2C3 conformers composed of $A\beta_{42}$, not $A\beta_{40}$, are significantly higher in AD patients than in NCs ($P = 0.0103$; Fig. 1E). Noticeably, the O/M index for either $A\beta_{42}$ or $A\beta_{40}$ is significantly higher in AD patients than in NCs: $A\beta_{42}$ O/M index ($P = 0.0012$) vs. $A\beta_{40}$ O/M index ($P = 0.0051$; Fig. 1F). Recently, Fukumoto et al. (2010) reported a similar finding, supporting the reliability of our finding. Another group also reported that the levels of AβOs in CSF are significantly higher in AD patients than in NCs (Georganopoulou et al., 2005). Along with with our findings, it is likely that the conversion of lipoprotein-free monomeric soluble Aβ into oligomeric assembly preferentially occurs in AD CSF, mirroring the disease-related metabolic conditions in the brain parenchyma. In support of our findings, a similar AD-related environmental alteration in CSF has been suggested (Ikeda et al., 2010). In contrast, it has been hypothesized that lower CSF $A\beta_{42}$ levels in AD patients can be ascribed to sequestration of soluble $A\beta_{42}$ into amyloid plaques. Several lines of evidence support this hypothesis; for example, an inverse correlation was found between CSF $A\beta_{42}$ levels and brain amyloid burden as evaluated by Pittsburgh compound B (PIB)-PET imaging (Klunk et al., 2004; Fagan et al., 2006). We have clarified this issue by comparing the levels of lipoprotein-free sAβMs in lipoprotein-depleted CSF from the 12 sporadic AD patients and 13 NCs. In the case of whole CSF, the relative amounts of sAβMs were similar in both groups (Fig. 3A). The LPD-CSF total AβM

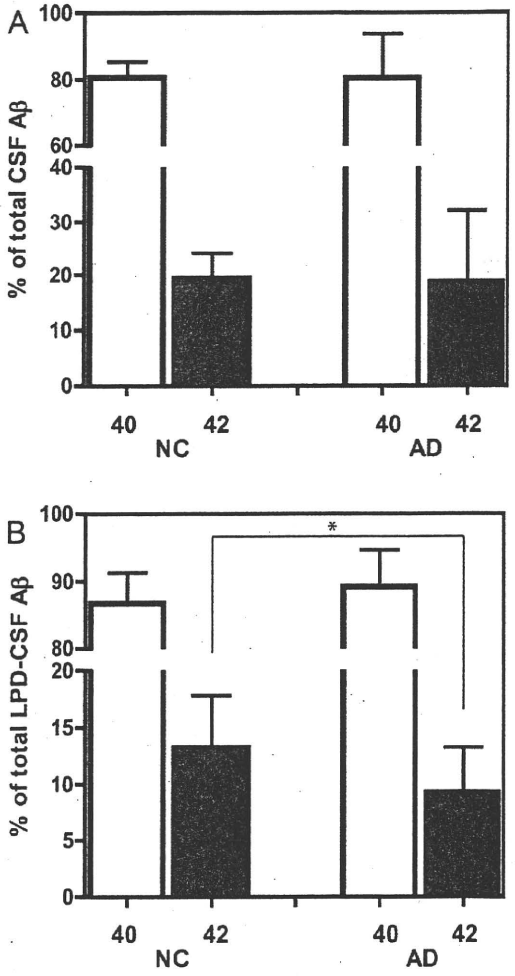

Fig. 3. Quantitation of $A\beta_{40}$ and $A\beta_{42}$ in native and lipoprotein-depleted CSF. The relative amounts (mean ± SD expressed as the percentage of total Aβ) of $A\beta_{40}$ (open bars) and $A\beta_{42}$ (solid bars) were quantitated in whole CSF (**A**) and lipoprotein-depleted CSF (**B**) in age-matched controls (NCs) and patients with sporadic Alzheimer's disease (AD). The levels of soluble Aβ species were measured by BNT-77-BA27 or BNT77-BC05 ELISA as described in Materials and Methods. Student's unpaired *t*-test revealed a statistically significant reduction (*$P = 0.0305$) in the relative amount of lipoprotein-free $A\beta_{42}$ in sporadic AD patients.

ID: AlexandarR Date: 17/2/11 Time: 03:22 Path: N:/3b2/JNR#/Vol00000/110029/APPFile/JW-JNR#110029

levels in both groups were relatively constant (302.8 ± 203.1 fmol/ml in sporadic AD patients and 463.9 ± 332.4 fmol/ml in NCs). In relative terms, the LPD-CSF AβMs values represented 31.6% ± 20.7% of the total Aβ in sporadic AD patients and 32.2% ± 13.5% of the total AβMs in NCs. Although these relative amounts of total lipoprotein-associated sAβMs (~70%) vs. lipoprotein-free sAβMs (~30%) remained essentially unchanged in sporadic AD patients, the amount of lipoprotein-free $A\beta_{42}$ was significantly lower ($P = 0.0305$) in the sporadic AD patients (9.3% ± 3.9%) than in NCs (13.2% ± 4.5%; Fig. 3B), which is in accordance with our above-mentioned finding that the level of oligomeric 2C3 conformers composed of $A\beta_{42}$ was significantly elevated in AD patients ($P = 0.0103$; see Fig. 2E). Note that about 70% of CSF sAβMs are normally associated with lipoprotein particles, whereas ~90% of sAβMs that circulate in normal plasma are associated with lipoprotein particles (Matsubara et al., 1999). These findings clearly indicate that the CNS constitutes a risky environment in which the lipoprotein–sAβMs interaction is impaired, leading to Aβ assembly. From this point of view, a key molecule to maintain monomeric $sA\beta_{42}$ metabolism in CNS appears to be HDL-like lipoprotein particles. A similar intracerebral sequestration of sAβMs by an anti-Aβ antibody has been proposed to prevent the accumulation of toxic Aβ assemblies (Yamada et al., 2009). In the case of HDL, a previous study showed that Aβ depositions is enhanced in PDAPP transgenic mice under conditions of markedly suppressed HDL (Wahrle et al., 2005), whereas Aβ depositions is inhibited in PDAPP transgenic mice under conditions of markedly overexpressed HDL (Wahrle et al., 2008). ApoE4-HDL shows less cholesterol exchange between lipid particles and the neuronal membrane compared with apoE3-HDL (Zou et al., 2002), leading to altered membrane functions, e.g., signal transduction, enzyme activities, ion channel properties, and conformation of sAβ peptides, which contribute to the disease-related metabolic conditions. In this sense, the dissociation of $sA\beta_{42}$ from or the lack of association with HDL-like lipoprotein particles not only constitutes a potential mechanism to initiate and/or accelerate the cascade favoring $A\beta_{42}$ assembly in the brain, but also results in a reduced clearance of physiological lipoprotein-associated $sA\beta_{42}$ peptides in the brain.

ACKNOWLEDGMENTS

We acknowledge Dr. Hui Sun for her participation in the early stages of this project.

REFERENCES

Chromy BA, Nowak RJ, Lambert MP, Viola KL, Chang L, Velasco PT, Jones BW, Fernandez SJ, Lacor PN, Horowitz P, Finch CE, Krafft GA, Klein WL. 2003. Self-assembly of $A\beta_{1-42}$ into globular neurotoxins. Biochemistry 42:12749–12760.

Cleary JP, Walsh DM, Hofmeister JJ, Shankar GM, Kuskowski MA, Selkoe DJ, Ashe KH. 2005. Natural oligomers of the amyloid-β protein specifically disrupt cognitive function. Nat Neurosci 8:79–84.

Enya M, Morishima-Kawashima M, Yoshimura M, Shinkai Y, Kusui K, Khan K, Games D, Schenk D, Sugihara S, Yamaguchi H, Ihara Y. 1999. Appearance of sodium dodecyl sulfate-stable amyloid beta-protein (Abeta) dimer in the cortex during aging. Am J Pathol 154:271–279.

Fagan AM, Mintun MA, Mach RH, Lee SY, Dence CS, Shah AR, LaRossa GN, Spinner ML, Klunk WE, Mathis CA, DeKosky ST, Morris JC, Holtzman DM. 2006. Inverse relation between in vivo amyloid imaging load and cerebrospinal fluid Abeta42 in humans. Ann Neurol 59:512–519.

Fukumoto H, Tokuda T, Kasai T, Ishigami N, Hidaka H, Kondo M, Allsop D, Nakagawa M. 2010. High-molecular-weight beta-amyloid oligomers are elevated in cerebrospinal fluid of Alzheimer patients. FASEB J 24:2716–2726.

Funato H, Enya M, Yoshimura M, Morishima-Kawashima M, Ihara Y. 1999. Presence of sodium dodecyl sulfate-stable amyloid beta-protein dimers in the hippocampus CA1 not exhibiting neurofibrillary tangle formation. Am J Pathol 155:23–28.

Georganopoulou DG, Chang L, Nam JM, Thaxton CS, Mufson EJ, Klein WL, Mirkin CA. 2005. Nanoparticle-based detection in cerebral spinal fluid of a soluble pathogenic biomarker for Alzheimer's disease. Proc Natl Acad Sci U S A 102:2273–2276.

Geula C, Wu CK, Saroff D, Lorenzo A, Yuan M, Yankner BA. 1998. Aging renders the brain vulnerable to amyloid beta-protein neurotoxicity. Nat Med 4:827–831.

Gong JS, Sawamura N, Zou K, Sakai J, Yanagisawa K, Michikawa M. 2002. Amyloid beta-protein affects cholesterol metabolism in cultured neurons: implications for pivotal role of cholesterol in the amyloid cascade. J Neurosci Res 70:438–446.

Gong Y, Chang L, Viola KL, Lacor PN, Lambert MP, Finch CE, Krafft GA, Klein WL. 2003. Alzheimer's disease-affected brain: presence of oligomeric Aβ ligands (ADDLs) suggests a molecular basis for reversible memory loss. Proc Natl Acad Sci U S A 100:10417–10422.

Hass C, Selkoe DJ. 2007. Soluble protein oligomers in neurodegeneration: lessons from the Alzheimer's amyloid β-peptide. Nat Rev Mol Cell Biol 8:101–112.

Ikeda T, Ono K, Elashoff D, Condron MM, Noguchi-Shinohara M, Yoshita M, Teplow DB, Yamada M. 2010. Cerebrospinal fluid from Alzheimer's disease patients promotes amyloid beta-protein oligomerization. J Alzheimers Dis 21:81–86.

Katsuno T, Morishima-Kawashima M, Saito Y, Yamanouchi H, Ishiura S, Murayama S, Ihara Y. 2005. Independent accumulations of tau and amyloid beta-protein in the human entorhinal cortex. Neurology 64:687–692.

Kayed R, Pensalfini A, Margol L, Sokolov Y, Sarsoza F, Head E, Hall J, Glabe C. 2009. Annular protofibrils are a structurally and functionally distinct type of amyloid oligomer. J Biol Chem 284:4230–4237.

Klein WL, Krafft GA, Finch CE. 2001. Targeting small Abeta oligomers: the solution to an Alzheimer's disease conundrum? Trends Neurosci 24:219–224.

Klunk WE, Engler H, Nordberg A, Wang Y, Blomqvist G, Holt DP, Bergström M, Savitcheva I, Huang GF, Estrada S, Ausén B, Debnath ML, Barletta J, Price JC, Sandell J, Lopresti BJ, Wall A, Koivisto P, Antoni G, Mathis CA, Långström B. 2004. Imaging brain amyloid in Alzheimer's disease with Pittsburgh compound-B. Ann Neurol 55:306–319.

Koudinov AR, Koudinova NV, Kumar A, Beavis RC, Ghiso J. 1996. Biochemical characterization of Alzheimer's soluble amyloid beta protein in human cerebrospinal fluid: association with high density lipoproteins. Biochem Biophys Res Commun 223:592–597.

Lacor PN, Buniel MC, Chang L, Fernandez SJ, Gong Y, Viola KL, Lambert MP, Velasco PT, Bigio EH, Finch CE, Krafft GA, Klein WL. 2004. Synaptic targeting by Alzheimer's-related amyloid β oligomers. J Neurosci 24:10191–10200.

Lambert MP, Barlow AK, Chromy BA, Edwards C, Freed R, Liosatos M, Morgan TE, Rozovsky I, Trommer B, Viola KL, Wals P, Zhang C, Finch CE. 1998. Diffusible, nonfibrillar ligands derived from $A\beta_{1-42}$ are potent central nervous system neurotoxins. Proc Natl Acad Sci U S A 95:6448–6453.

Lashuel HA, Hartley D, Petre BM, Walz T, Lansbury PT Jr. 2002. Neurodegenerative disease: amyloid pores from pathogenic mutations. Nature 418:291.

Lesné S, Koh MT, Kotilinek L, Kayed R, Glabe CG, Yang A, Gallagher M, Ashe KH. 2006. A specific amyloid-beta protein assembly in the brain impairs memory. Nature 440:352–357.

Lin H, Bhatia R, Lal R. 2001. Amyloid beta protein forms ion channels: implications for Alzheimer's disease pathophysiology. FASEB J 15:2433–2444.

Matsubara E, Ghiso J, Frangione B, Amari M, Tomidokoro Y, Ikeda Y, Harigaya Y, Okamoto K, Shoji M. 1999. Lipoprotein-free amyloidogenic peptides in plasma are elevated in patients with sporadic Alzheimer's disease and Down's syndrome. Ann Neurol 45:537–541.

Matsubara E, Sekijima Y, Tokuda T, Urakami K, Amari M, Shizuka-Ikeda M, Tomidokoro Y, Ikeda M, Kawarabayashi T, Harigaya Y, Ikeda S, Murakami T, Abe K, Otomo E, Hirai S, Frangione B, Ghiso J, Shoji M. 2004. Soluble Abeta homeostasis in AD and DS: impairment of anti-amyloidogenic protection by lipoproteins. Neurobiol Aging 25:833–841.

Michikawa M, Gong JS, Fan QW, Sawamura N, Yanagisawa K. 2001. A novel action of alzheimer's amyloid beta-protein (Abeta): oligomeric Abeta promotes lipid release. J Neurosci 21:7226–7235.

Noguchi A, Matsumura S, Dezawa M, Tada M, Yanazawa M, Ito A, Akioka M, Kikuchi S, Sato M, Ideno S, Noda M, Fukunari A, Muramatsu S, Itokazu Y, Sato K, Takahashi H, Teplow DB, Nabeshima Y, Kakita A, Imahori K, Hoshi M. 2009. Isolation and characterization of patient-derived, toxic, high mass amyloid beta-protein (Abeta) assembly from Alzheimer disease brains. J Biol Chem 284:32895–32905.

Quist A, Doudevski I, Lin H, Azimova R, Ng D, Frangione B, Kagan B, Ghiso J, Lal R. 2005. Amyloid ion channels: a common structural link for protein-misfolding disease. Proc Natl Acad Sci U S A 102:10427–10432.

Schmechel DE, Saunders AM, Strittmatter WJ, Crain BJ, Hulette CM, Joo SH, Pericak-Vance MA, Goldgaber D, Roses AD. 1993. Increased amyloid beta-peptide deposition in cerebral cortex as a consequence of apolipoprotein E genotype in late-onset Alzheimer disease. Proc Natl Acad Sci U S A 90:9649–9653.

Selkoe DJ. 2002. Alzheimer's disease is a synaptic failure. Science 298:789–791.

Shankar GM, Li S, Mehta TH, Garcia-Munoz A, Shepardson NE, Smith I, Brett FM, Farrell MA, Rowan MJ, Lemere CA, Regan CM, Walsh DM, Sabatini BL, Selkoe DJ. 2008. Amyloid-betaprotein dimers isolated directly from Alzheimer's brains impairsynaptic plasticity and memory. Nat Med 14:837–842.

Tanzi RE, Bertram L. 2001. New frontiers in Alzheimer's disease genetics. Neuron 32:181–184.

Wahrle SE, Jiang H, Parsadanian M, Hartman RE, Bales KR, Paul SM, Holtzman DM. 2005. Deletion of Abca1 increases Abeta deposition in the PDAPP transgenic mouse model of Alzheimer disease. J Biol Chem 280:43236–43242.

Wahrle SE, Jiang H, Parsadanian M, Kim J, Li A, Knoten A, Jain S, Hirsch-Reinshagen V, Wellington CL, Bales KR, Paul SM, Holtzman DM. 2008. Overexpression of ABCA1 reduces amyloid deposition in the PDAPP mouse model of Alzheimer disease. J Clin Invest 118:671–682.

Walsh DM, Klyubin I, Fadeeva JV, Cullen WK, Anwyl R, Wolfe MS, Rowan MJ, Selkoe DJ. 2002. Naturally secreted oligomers of amyloid β protein potently inhibit hippocampal long-term potentiation in vivo. Nature 16:535–539.

Wellington CL. 2004. Cholesterol at the crossroads: Alzheimer's disease and lipid metabolism. Clin Genet 66:1–16.

Yamada K, Yabuki C, Seubert P, Schenk D, Hori Y, Ohtsuki S, Terasaki T, Hashimoto T, Iwatsubo T. 2009. Abeta immunotherapy: intracerebral sequestration of Abeta by an anti-Abeta monoclonal antibody 266 with high affinity to soluble Abeta. J Neurosci 29:11393–11398.

Zou K, Gong JS, Yanagisawa K, Michikawa M. 2002. A novel function of monomeric amyloid beta-protein serving as an antioxidant molecule against metal-induced oxidative damage. J Neurosci 22:4833–4841.

Journal of Neuroscience Research

Journal of Neuroscience Research 89:576–584 (2011)

Factors Responsible for Neurofibrillary Tangles and Neuronal Cell Losses in Tauopathy

Yasuhito Wakasaya,[1] Takeshi Kawarabayashi,[1]* Mitsunori Watanabe,[1] Yukiko Yamamoto-Watanabe,[1] Ayumi Takamura,[1] Tomoko Kurata,[2] Tetsuro Murakami,[2] Koji Abe,[2] Kiyofumi Yamada,[3] Koichi Wakabayashi,[4] Atsushi Sasaki,[5] David Westaway,[6] Peter St. George Hyslop,[7] Etsuro Matsubara,[1] and Mikio Shoji[1]

[1]Department of Neurology, Institute of Brain Science, Hirosaki University Graduate School of Medicine, Hirosaki, Japan
[2]Department of Neurology, Okayama University Graduate School of Medicine, Dentistry and Pharmaceutical Sciences, Okayama, Japan
[3]Department of Neuropsychopharmacology and Hospital Pharmacy, Nagoya University Graduate School of Medicine, Nagoya, Japan
[4]Department of Neuropathology, Institute of Brain Science, Hirosaki University Graduate School of Medicine, Hirosaki, Japan
[5]Department of Pathology, Saitama Medical University, Saitama, Japan
[6]Centre for Prions and Protein Folding Diseases, 204 Environmental Engineering Building, University of Alberta, Edmonton, Alberta, Canada
[7]Centre for Research in Neurodegenerative Diseases, Departments of Medicine (Neurology) and Laboratory Medicine and Pathobiology, University of Toronto, Toronto, Ontario, Canada

TgTauP301L mice that overexpress the mutant human tauP301L present in FTDP-17 reproduce neurofibrillary tangles (NFTs), neuronal cell losses, memory disturbance, and substantial phenotypic variation. To demonstrate factors responsible for NFT formation and neuronal cell losses, sets of TgTauP301L for comparison with or without NFTs and neuronal cell losses were studied with oligonucleotide microarrays. Gene expressions were altered in biological pathways, including oxidative stress, apoptosis, mitochondrial fatty acid betaoxidation, inflammatory response pathway, and complement and coagulation cascade pathways. Among 24 altered genes, increased levels of apolipoprotein D (ApoD) and neuronal PAS domain protein 4 (Npas4) and decreased levels of doublecortin (DCX) and potassium channel, voltage-gated, shaker-related subfamily, β member 1 (Kcnab1) were found in the TgTauP301L with NFTs and neuronal cell losses, Alzheimer's brains, and tauopathy brains. Thus, many biological pathways and novel molecules are associated with NFT formation and neuronal cell losses in tauopathy brains. © 2011 Wiley-Liss, Inc.

Key words: tauopathy; Apo D; Npas4; DCX; Kcnab1

Alzheimer's disease (AD) brains are invariably characterized by two pathological features: initial Aβ amyloidosis by extracellular deposition of Aβ, and subsequent tauopathy with intracellular accumulation of neurofibrillary tangles (NFTs) comprising abnormal aggregates of phosphorylated tau. Aβ cascade from Aβ deposits to the final appearance of NFTs and neuronal cell losses is the major hypothesis that explains all steps in the pathogenesis of AD (Hardy, 2009). Although soluble Aβ oligomers are cardinal molecules that adversely affect synaptic structures and plasticity, leading to memory disturbance, neuronal cell loss is closely related to the presence of NFTs (Spires-Jones et al., 2009). Accumulation of tau in axonal defects is an early event in AD brain and in APP transgenic mouse (Stokin et al., 2005). Suppression of tau expression in mice expressing a repressible tauP301L and developing progressive NFTs, neuronal cell losses, and behavior

Contract grant sponsor: Ministry of Health, Labor and Welfare of Japan (to M.S.); Contract grant sponsor: Ministry of Education, Culture, Sports, Science and Technology, Japan; Contract grant number: 19390233 (to M.S.); Contract grant number: 19590976 (to T.K.); Contract grant number: 18590968 (to E.M.); Contract grant sponsor: The Mochida Memorial Foundation for Medical and Pharmaceutical Research (to M.W.); Contract grant sponsor: Hirosaki University Institutional Research (to M.S.).

*Correspondence to: Dr. Takeshi Kawarabayashi, Department of Neurology, Institute of Brain Science, Hirosaki University Graduate School of Medicine, 5 Zaifucho, Hirosaki 036-8562, Japan.
E-mail: tkawara@cc.hirosaki-u.ac.jp

Received 1 September 2010; Revised 8 November 2010; Accepted 9 November 2010

Published online 13 January 2011 in Wiley Online Library (wileyonlinelibrary.com). DOI: 10.1002/jnr.22572

impairments recovered memory function and neuron numbers (Santacruz et al., 2005). However, once NFTs are formed, these features are irreversible (Holmes et al., 2008). Transgenic tau zebrafish have clearly shown that GSK3β-mediated NFT formation actually induces neuronal cell losses (Paquet et al., 2009). These findings support the hypothesis that tauopathy is the critical event in neuronal cell losses in AD and frontotemporal dementia (FTD) patients. In FTD and parkinsonism linked to chromosome 17 (FTDP-17), there is large variation in the clinical and neuropathological features of disease among patients showing the same mutation within a family. We recently established a tauopathy model mouse expressing 2N4R human tauP301L, developing florid pathology, including numerous pretangles, NFTs, glial fibrillary tangles (GFTs), gliosis, and neuronal cell losses in the frontotemporal areas of the cerebrum accompanied by cerebral atrophy (TgTauP301L; Murakami et al., 2006). As expected, TgTauP301L also showed variation in phenotypic manifestation. Given that the genetic modifiers or associated molecules are clarified by comparison between individuals showing severe pathology including numerous NFTs and neuronal cell losses and those with only pretangles, study of the variance both in families with FTDP-17 and in our mouse model can contribute to clarifying the pathological cascade from accumulation of phosphorylated tau to NFT formation and final neuronal cell losses. On the basis of this hypothesis, here we analyzed oligonucleotide microarrays to determine the mRNA expression profile in TgTauP301L with and without tau pathology and showed the alterations of biological pathways and novel proteins associated with NFTs and neuronal cell losses.

MATERIALS AND METHODS

Subjects

TgTauP301L were back-crossed to FVB/N strain mice for more than six generations to obtain a uniform genetic background. Two sets of TgTauP301L consisted of the 517 mouse with human tau accumulation (Fig. 1Ba–e) and the 512 mouse showing extensive NFTs and neuronal cell losses (Fig. 1Bf–j), which were compared at 24 months of age, as well as the 739 mouse with only human tau accumulation (Fig. 1Aa,b, Bk–o) and the 736 mouse showing extensive NFTs and neuronal cell losses (Fig. 1Ac,d, Bp–t), which were compared at 26 months of age, using oligonucleotide microarrays. After mice were sacrificed under ether anesthesia, the sagittal half of the brain was immediately frozen at −80°C for Western blot and microarray analysis, and the other half of the brain was analyzed histologically. An additional 185 TgTauP301L between 3 months and 30 months of age, 52 nontransgenic control littermates (3–30 months old), and autopsy brains from five patients with Alzheimer's disease (ages 65–81 years), five patients with tauopathy [two frontotemporal dementia (FTD), two corticobasal degeneration, and one supranuclear palsy (ages 71–78 years)], and five normal controls (ages 71–91 years) were examined by immunostaining and biochemical analysis.

Target RNA Preparation and Oligonucleotide Array Expression Analysis

Total RNAs from two sets of mouse brains were isolated using the Trizol reagent (Invitrogen, Carlsbad, CA) and purified with a RNeasy Mini Kit (Qiagen, Valencia, CA). The One-Cycle cDNA synthesis kit from Affymetrix was used to synthesize cDNA from 2 μg of total RNA. Biotinylated cRNA was generated from the cDNA using the IVT Labeling Kit (Affymetrix, Santa Clara, CA), followed by fragmentation of the cRNA target using a fragmentation buffer for 35 min at 94°C before chip hybridization, then 15 μg of fragmented cRNA was added to a hybridization cocktail (0.05 μg/μl fragmented cRNA, 50 pM control oligonucleotide B2, 1.5 pM *BioB*, 5 pM *BioC*, 25 pM *BioD*, and 100 pM *cre* hybridization controls, 0.1 mg/ml herring sperm DNA, 0.5 mg/ml acetylated BSA, 100 mM MES, 1 M Na^+, 20 mM EDTA, 0.01% Tween 20). Ten micrograms of cRNA from each sample was hybridized to a separate oligonucleotide array (Affymetrix Mouse Genome 430 2.0) for 16 hr at 45°C in the GeneChip Hybridization Oven 640. The arrays were washed and stained with streptavidin phycoerythrin in the GeneChip Fluidics Station 450. Then, the arrays were scanned with a GeneChip Scanner 3000.

Data Analysis

The Affymetrix GeneChip Microarray Suite 5.0 (MAS5) algorithm was used to generate signal values and detection calls (present, absent or marginal). Only genes that had a "present" or "marginal" detection call on all four chips were chosen, with 24,330 identified for further analysis from a total of 45,101 genes. Ratios of changes in gene expression were obtained by the differences between 517 and 512 and between 739 and 736. Gene expression ratios of ≥ 2 or ≤ 0.5 were chosen as cutoff values, defining increased and decreased expression, respectively. Filtered genes identified as differentially expressed by twofold or greater in both comparisons were tested for statistical significance using moderated *t* statistics by the empirical Bayes method in the R package "limma" (Smyth, 2004). For moderated *t*-test, we choose a threshold of $P < 0.05$. The corresponding false-discovery rate was 0.076, meaning that 7.6% of the genes selected by this *P* value could be false-positive (Benjamini and Hochberg, 1995).

For biological interpretation of the differentially expressed genes, the number of appearances of each gene ontology (GO) term (http://www.geneontology.org/) was counted from each list of genes. Fisher's exact test to assess the significance for enrichment of genes within three kinds of GO categories (BP, biological process; MF, molecular function; CC, cellular component) in a list was performed by the GO Browser tool in GeneSpring GX 7.3.1 (Agilent Technologies, Santa Clara, CA).

We also performed a pathway analysis with parametric analysis of gene-set enrichment (PAGE; Kim and Volsky, 2005) to analyze the differential expression of predefined gene sets rather than individual genes. This test was implemented by calculating a Z score for a given gene set that measures the deviation of the average log-ratio for genes in the category

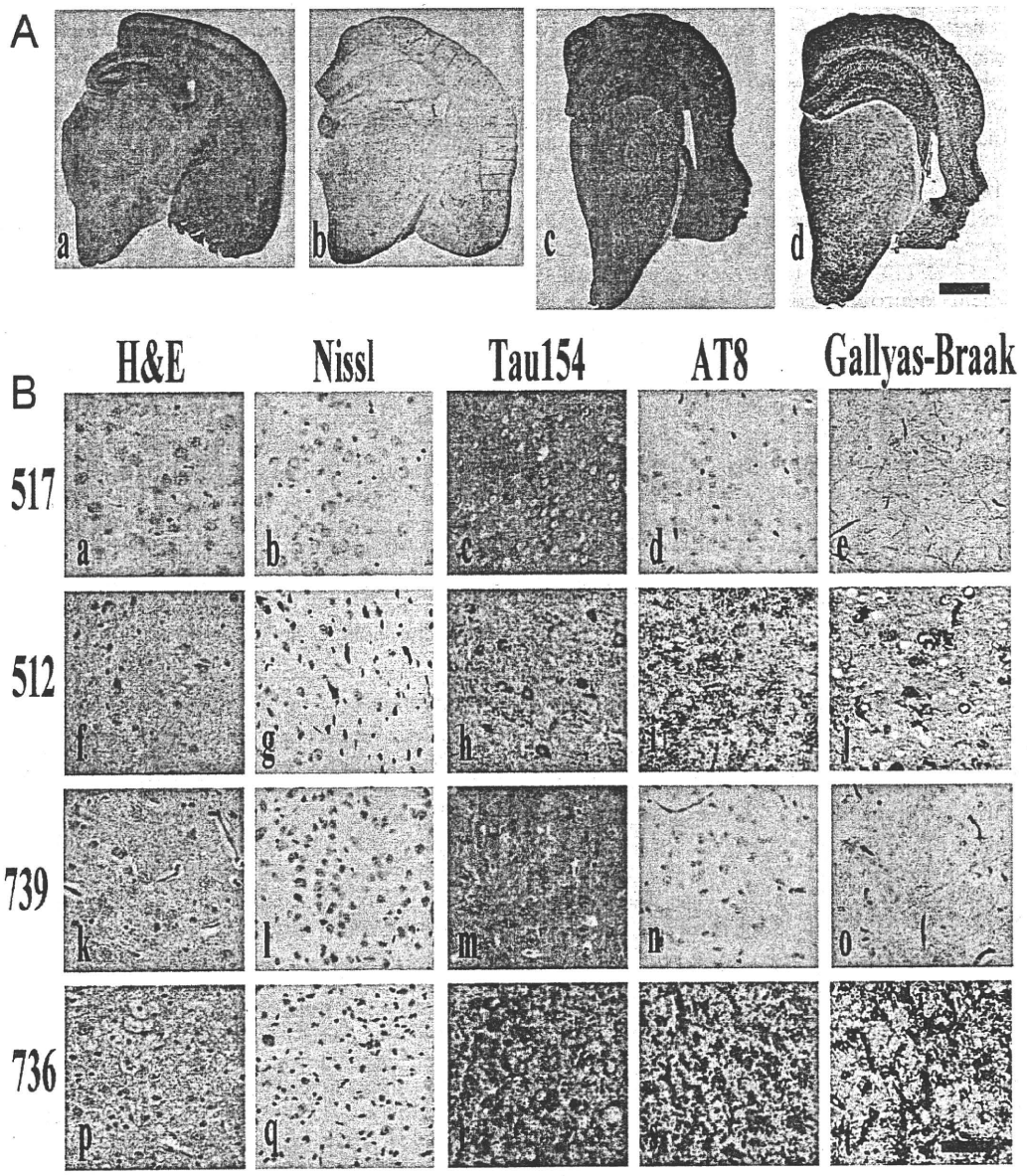

Fig. 1. Phenotypic variation in TgTauP301L mice. **A**: Brains of 739 (a,b) and 736 (c,d); a and c show tau154 staining, and b and d show Gallyas-Braak silver staining. Accumulation of human tauP301L was similar between 739 and 736. However, severe NFTs and brain atrophy were prominent in 736 (d). **B**: Brain sections of 517, 512, 739, and 736 were stained with hematoxylin and eosin (H&E; a,f,k,p), Nissl (b,g,l,q), tau154 antibody (c,h,m,r), AT8 antibody (d,i,n,s), and Gallyas-Braak silver staining (e,j,o,t). Neuronal cell losses and NFT formation were prominent in 512 (g,j) and 736 (q,t). Scale bar = 1 mm in A; 50 μm in B. [Color figure can be viewed in the online issue, which is available at wileyonlinelibrary.com.]

from the genome-wide average, in units of the standard deviation. The Z score for each category was calculated as

$$Z = (\bar{X} - \mu)\sigma/\sqrt{n},$$

where μ and σ represent the mean and the standard deviation of total -fold change values of genes after filtering by MAS5 detection call, respectively. $\bar{X}$ is the mean of -fold change values of genes for a given set, and n is the size of a given gene set. The predefined gene sets were created from GenMAPP (http://www.genmapp.org/).

Immunostaining

Tissues were fixed in 4% paraformaldehyde with 0.1 M phosphate buffer (pH 7.6) for 8 hr and embedded in paraffin. Five-micrometer-thick sections were prepared for immuno-

staining and Gallyas-Braak silver stain. For tau immunostaining, sections were immersed in 0.5% periodic acid for blocking intrinsic peroxidase and treated with 99% formic acid for 3 min. After blocking with 5% normal goat or horse serum, sections were incubated overnight with primary antibodies. The specific labeling was visualized using Vectastain Elite ABC kit (Vector, Burlingame, CA). Tissue sections were counterstained with hematoxylin. The following antibodies were used for immunostaining: tau154 (1:200), TAU-5 (1:1,000; Biosource. Camarillo, CA), AT8 (1:400; Innogenetics, Gent, Belgium; Murakami et al., 2006), antibodies to ApoD (1:1,000; Patel et al., 1995; 36C6, 1:100; Novocastra Laboratories, Newcastle, United Kingdom), antibodies to DCX (N-19, 1:200; C-18, 1:200; Santa Cruz Biotechnology, Santa Cruz, CA), antibody to Npas4 (1: 50, polyclonal antibody to purified Npas4; 1:100, NBP1-06574; Novus Biologicals, Littleton, CO), and antibody to Kcnab1 (1: 50; Santa Cruz Biotechnology).

Western Blotting

The remaining brain sample was homogenized in 9 volumes of Tris-saline buffer with protease inhibitors (Complete Inhibitor Cocktail tablets; Roche, Mannheim, Germany) and centrifuged at 55,000 rpm for 60 min at 4°C (TS buffer-soluble fraction). The pellet was homogenized again in 4 volumes of 1% sarkosyl in TS, incubated on ice for 30 min, and centrifuged at 55,000 rpm for 60 min at 4°C. The pellet was analyzed as the sarkosyl-insoluble fraction. The samples were boiled at 70°C in 4 volumes of SDS sample buffer, separated on 4–12% NuPAGE Bis-Tris Gel (Invitrogen, Carlsbad, CA), and the blots were labeled by antibodies. Signals were visualized with an enhanced chemiluminescence detection system (Pierce United Kingdom) and quantified by a lumino-image analyzer (LAS 1000-mini; Fuji Film, Tokyo, Japan). The signals were corrected by those of β-actin, and were tested for statistical significance using *t*-tests [TgTauP301L with NFTs and neuronal cell losses (n = 3) and without NFTs and neuronal cell losses (n = 3)]. All animal experiments were performed according to guidelines established in the *Guide for the care and use of laboratory animals* and by the ethical committee of Hirosaki University.

RESULTS

In comparing gene expression ratios between 517 and 512, 278 were increased and 162 were decreased. There were 477 increased gene expression ratios and 369 decreased gene expression ratios between 739 and 736. In the two comparisons of gene expression ratios, there were 52 up-regulations and 16 down-regulations in common. Among these 68 gene expressions, 37 gene expressions were significant, and 24 genes have already been described (Table I). There was no alteration of gene expression ratios for APP, MAPT, or GSK3β in 517, 512, 739, and 736 mouse brains.

According to biological pathways and gene expression groupings based on the GenMAPP database, comparison between 517 and 512 demonstrated seven down-regulated gene expression ratio groups. Five pathways consisted of up-regulated gene expression ratio groups. On comparison between 739 and 736, only one pathway showed a down-regulated gene expression group; however, 41 pathways showed up-regulated gene expression groups. Among these biological pathways, inflammatory response, mitochondrial fatty acid beta-oxidation, oxidative stress, apoptosis, and complement and coagulation cascades were commonly up-regulated.

To confirm further the differences in gene expression profile associated with NFT formation and neuronal cell losses, ApoD (Muffat and Walker, 2010), Npas4 (Lin et al., 2008), DCX (Moores et al., 2004), and Kcnab1 (Need et al., 2003) were selected for analysis at the protein level of up- or down-regulated genes among 24 significant genes because of the availability of antibodies. ApoD and DCX gene products had been previously suggested to be altered in AD (Thomas et al., 2003; Jin et al., 2004); however, others have not been reported.

On immunostaining, ApoD was markedly labeled in the brain of TgTauP301L with NFTs and neuronal cell losses compared with those of TgTauP301L without NFTs and neuronal cell losses. In particular, the hippocampus and white matter were markedly stained (Fig. 2b). Enhanced ApoD immunostaining was not detected in brains of TgTauP301L without NFTs and neuronal cell losses (Fig. 2a). The areas that exhibited extensive ApoD immunoreactivities were not related to those showing NFT formation and neuronal cell losses. Increased ApoD immunostaining was detected in neuronal processes, oligodendrocytes, and astrocytes (Fig. 2d) compared with that in 739 brains (Fig. 2c). Astrocytosis was also prominent in these areas. In AD and tauopathy brains, ApoD immunostaining was also detected mainly in astrocytes of the white matter and rarely in neurons in the cortex (Fig. 2f,g,i,j). ApoD was not detected in the control normal human brains (Fig. 2e,h).

Markedly decreased DCX immunoreactivities were observed in TgTauP301L showing NFTs and neuronal cell losses (Fig. 2l,n). Decrease in DCX-positive cells was observed even in areas without NFT formation. DCX-positive cells were detected in the dentate gyrus, hippocampus, and cerebral cortex of age-matched control nontransgenic mouse and TgTauP301L without NFTs and neuronal cell losses. Band-like immunoreactivities were prominent in the hippocampus of control age-matched nontransgenic mice (Fig. 2k,m). In AD and tauopathy brains, reticular immunoreactivity of DCX was markedly decreased in the dentate gyrus (Fig. 2p,q,s,t) compared with that in control human brains (Fig. 2o,r).

On Western blotting, the amount of DCX was decreased and the level of ApoD was increased in TgTauP301L mice with NFTs and neuronal cell losses compared with those in TgTauP301L without NFTs and neuronal cell losses (Fig. 3). The amounts of DCX and ApoD in sarkosyl-soluble fraction of the brain were correlated with the amount of sarkosyl-insoluble tau of the brain, suggesting that down-regulation of DCX and up-regulation of ApoD were closely associated with